A game-theoretical modeling framework for spectrum markets and cognitive-radio devices

Georgios Fortetsanakis
Department of Computer Science
University of Crete &
ICS-FORTH

Markos Katsoulakis
Department of Applied Mathematics
University of Crete &
IACM-FORTH

Maria Papadopouli
Department of Computer Science
University of Crete &
ICS-FORTH

***Abstract*—This report presents a novel game-theoretical framework to model the evolution of spectrum markets that consists of multiple spectrum/network operators that provide wireless access to users. It integrates models about the channel, mobility, user preference, network operators (providers), infrastructure deployment, user distribution, and price-adaptation mechanisms. Providers aim to maximize their own profit, while clients decide based on criteria, such as the financial cost of the access, transmission rate and required transmission power. This work discusses briefly the modeling framework and a novel price-adaptation algorithm for providers. It presents how this framework can be used to instantiate a cellular-based market in a small city. Finally, it analyzes the evolution of this market under different topologies and user profiles, summarizing the main performance results.**

I. Introduction

Cognitive radio networks (CRNs), an emerging disruptive technology, aims to improve spectrum utilization, enabling dynamic spectrum use. This research aims in the design of a complete *multi-layer* modeling framework of CRNs, incorporating both systems and business aspects using statistical mechanics, game theory and economics. It integrates models about the channel, network operators, infrastructure, and primary and secondary devices (e.g., their preference, constraints, placement). A distinct prominent feature is its emphasis on the interactions among the CRNs entities, that occur in *multiple time and spatial scales*. The multi-layer modeling aspect is inspired by the approach in [1]. We are in the process of developing a modular simulation environment that implements the modeling framework and instantiates various models, allowing comparative assessments of spectrum-sharing mechanisms under different scenarios. The framework should enable researchers to capture different types of *information sharing*, interactions, negotiation strategies, and *trust* among entities.

To the best of our knowledge, it is the only modeling framework that attempts to incorporate such an extensive set of parameters that allow the modeling of various complex interactions of CRNs entities and business-driven cases in a realistic manner. Most of the related approaches focus on a specific sub-problem/aspect of CRNs omitting their inherent features. Specifically, most research approaches can be classified into two categories, namely, the *microscopic-* and the *macroscopic*-level ones. The microscopic-level approaches consider interactions among secondary devices at a very fine spatial level, mostly assuming a limited number of primary devices due to the high computational complexity [2], [3], [4], [5], [6], [7], [8]. On the other hand, the macroscopic approaches focus on the revenue of the providers, considering only an "average" behavior (over large temporal or spatial scales) of secondary devices [9], [10], [11], [12]. Unlike these approaches, this framework models the interactions of primary and secondary entities at *various spatial scales*, from large metropolitan areas to small neighborhoods, enabling the instantiation of various parameters at *different time granularities*. For example, the rate at which primary devices change their prices for their spectral resources is often smaller than the rate at which secondary devices demand for spectral resources.

An intuitive way to think of the multi-layer aspect in the modeling framework is as mathematical transformations that allow to "scale up or down" the modeling environment. At the microscopic level of the framework, the various entities are modeled in fine temporal and spatial detail. On the other hand, the mesoscopic level exhibits various *aggregations*. For example, the users are modeled as a *population* with certain attributes, computed as *spatial averages* of the characteristics of the individual users of that population. Furthermore, the selection process of these user populations are no longer deterministic but *stochastic* and *location-dependent*. Due to the heterogeneity of these populations, the framework allows the definition of mixed strategies for the spectrum access negotiation process. For example, in the case of a population of users, a mixed strategy indicates the probability with which users choose to buy spectrum from various providers at a specific location. Section II describes the modeling framework. Section III illustrates how this framework can be used to instantiate and assess a spectrum market with cellular-based network access and discusses our findings.

II. Modeling framework

A. General model

The most important parameters of the modeling framework are (a) the channel, (b) the network topology (e.g., cellular, mesh, vehicular), (c) the network operator infrastructure deployment/distribution, (d) the user mobility and distribution, (e) the relations and interactions among primary and secondary entities (e.g., among primary devices, between primary and secondary devices, among network operators), (f) the

multiple spatio-temporal scales (over which these relations and interactions are manifested), (g) the type, reliability and amount of information that is available to various entities, (h) the user preferences and tolerance criteria with respect to the wireless access (e.g., based on transmission rate, energy, financial cost, handoffs frequency, duration of disconnection) and the network operator selection mechanism, (i) the user profile (e.g., misconfigured/selfish/malicious entities), (j) the utility function of the primary entities (e.g., spectrum owner), and (k) price-adaptation algorithm.

The simulation environment based on this framework is modular, in that, it can instantiate and implement different models for the aforementioned parameters. For example, the channel can be modeled using large-scale propagation models (e.g., path-loss and shadowing) and smaller-scale models (e.g., fading).

This report simulated the cellular topologies of two network operators that offer wireless access via their base stations (BSs) to wireless users in a small city. The network operators (called also *providers*) are the primary entities that own a part of the spectrum, offering wireless access via their base stations (BSs). Secondary entities (called also *users*) buy the wireless Internet access from network operators for a certain duration. Furthermore, we assume that the providers divide their channels into time-frequency slots according to a TDMA scheme and that each user can utilize a single slot.

To simulate the channel quality we employed the *Okumura Hata* path-loss model for small cities [13]. Moreover, the contribution of shadowing (expressed in dB) to the channel gain at the positions of BSs follows a multivariate Gaussian distribution with mean $\mathbf{0}$ and covariance matrix defined in Eq. (1).

$$C(i,j) = \begin{cases} \sigma_s^2 & \text{if } i = j, \\ \sigma_s^2 e^{-\|L_i - L_j\|/X_c} & \text{if } i \neq j. \end{cases} \quad (1)$$

Where σ_s is the standard deviation of shadowing (2.5 dB in our simulations), X_c is the correlation distance within which the shadowing effects are correlated [14] and L_i, L_j are the positions of the BSs i and j respectively.

To model the effect of angular correlation of shadowing we represent each BS with six points instead of one. These points lie on a circle with center the BS position and radius 1m and they are equally spaced. Furthermore, we determine the value of shadowing at the points that represent all BSs by drawing a sample from the distribution described in Eq. (1). When a user communicates with a specific BS, the contribution of shadowing to the channel gain is equal to the value that corresponds to the point representing the BS, whose direction is the closest to the direction of arrival of the signal [15].

We compute the interference power at a time-frequancy slot belonging to a specific BS by measuring the contribution of all interfering users at cochannel BSs. Moreover, we assume that cochannel BSs of the same provider are not synchronized resulting in overlaps between multiple time-frequency slots and thus in users that interfere to more than one slots. In real wireless networks, the amount of interference at the available time-frequency slots and the channel gain will be measured by the network interfaces of BSs and sent to the users with appropriate messages. To penalize an aggressive increase of the transmission power (that may introduce harmful interference to other devices), the providers adopt a pricing scheme that charges the users proportionally to the transmission power they invest. Moreover, the maximum allowable transmission power that a user can invest is 2 Watts.

Considering that there is a set of users U in a particular geographical region, each user $u \in U$ takes its decisions by solving the following optimization problem.

$$\begin{aligned} \underset{\mathbf{T}_u}{\text{maximize}} \quad & \sum_{s \in S} a \left(\frac{B}{N}\right) \log_2 \left(1 + \frac{T_u(s) G(u,s)}{I(s)}\right) - bc(s) T_u(s) \\ \text{subject to} \quad & 0 \leq \sum_{s \in S} T_u(s) \leq T_{max} \\ & \sum_{s \in S} c(s) T_u(s) \leq C^u_{max} \\ & \sum_{s \in S} \left(\frac{B}{N}\right) \log_2 \left(1 + \frac{T_u(s) G(u,s)}{I(s)}\right) \geq R^u_{tar} \\ & \sum_{s \in S} sign(T_u(s)) = 1 \end{aligned}$$

Where S is the set of available time-frequency slots at all BSs, $G(u,s)$ is the channel gain that the user u observes at the time-frequency slot s and $I(s)$, $c(s)$ are the interference and noise power and monetary cost of the slot s respectively. B is the width of a single channel and N is the number of time-frequency in which a channel is divided. Furthermore, T_{max}, C^u_{max}, and R^u_{tar} are the maximum allowable transmission power, the maximum price per minute that the user u can tolerate for a time-frequency slot and the target transmission rate of the user u. Finally, the vector $\mathbf{T}_u = (T_u(s))_{s \in S}$ contains the transmission power that the user u invests in all available time-frequency slots and the function $sign(x)$ is defined as follows.

$$sign(x) = \begin{cases} 1 & \text{if } x > 0, \\ 0 & \text{otherwise} \end{cases} \quad (2)$$

The objective of the above optimization problem consists of two parts. The first part is the total achievable transmission rate while the second part is the monetary cost that is required to achieve this rate. Moreover, each of these parts is taken into consideration with a different weight(a and b respectively). The final constraint restricts each user to invest transmission power at a single time-frequency slot. To solve this problem we consider each time-frequency slot $s \in S$ separately and solve the following problem.

$$\underset{T_u(s)}{\text{maximize}} \quad a\left(\frac{B}{N}\right)\log_2\left(1+\frac{T_u(s)G(u,s)}{I(s)}\right)-bc(s)T_u(s)$$

$$\begin{aligned}\text{subject to} \quad & 0 \le T_u(s) \le T_{max} \\ & c(s)T_u(s) \le C^u_{max} \\ & \left(\frac{B}{N}\right)\log_2\left(1+\frac{T_u(s)G(u,s)}{I(s)}\right) \ge R^u_{tar}\end{aligned}$$

In other words, we compute the optimal value of the objective function for each time-frequency slot and subsequently we choose the slot whose optimal value is the largest. To decrease the computational complexity of the above procedure, we exclude the time-frequency slots that satisfy one of the following conditions.

$$c(s)T^l_u > C^u_{max} \quad (3a)$$

$$\left(\frac{B}{N}\right)\log_2\left(1+\frac{T^h_u G(u,s)}{I(s)}\right) < R^u_{tar} \quad (3b)$$

$$\frac{G(u,s)}{I(s)} < \max_{s'\in S}\frac{G(u,s')}{I(s')} \text{ and } c(s) > \min_{s'\in S} c(s') \quad (3c)$$

Where T^l_u is the minimum amount of transmission power required to achieve the target transmission rate and T^h_u is the minimum between T_{max} and the maximum transmission power for which the monetary cost constraint is satisfied. Slots that satisfy the condition (3a) can not satisfy the monetary cost constraint while slots that satisfy the condition (3b) can not satisfy the target transmission rate constraint. Finally, slots that satisfy the condition (3c) are characterized by channel conditions that are worse than the best channel conditions over all slots and a monetary cost that is larger than the minimum monetary cost over all slots and thus they can not be chosen.

In general, different service paradigms can be modeled (e.g., *"time/recharge" cards* or *subscription-based* schemes). Most of the related approaches consider a given (*a priori* known) function that models the demand of secondary users to perform the price adaptation or decide about the amount of spectrum, which providers will offer in a given market [9], [10], [11], [12]. Unlike them, this work does not assume that the demand is known. Moreover, it employs a price adaptation algorithm which assumes that the providers only know their own prices and the prices of their competitors and measure their own revenue. No knowledge is available about the user characteristics and preferences. This algorithm is described in subsection II-B although different algorithms may also be employed.

B. Price adaptation algorithm

We consider a spectrum market in which a set $P = \{p_1, p_2, ..., p_K\}$ of providers compete to offer services to end users. For each possible combination of prices $\mathbf{x} = (x_1, x_2, ..., x_K)$ that are offered, each provider $p \in P$ achieves the revenue $F_p(\mathbf{x})$. The function $F_p : R^{K+} \to R$ is generally unknown due to the limited information that is available to each provider. Furthermore, in some scenarios, this function may be time-varying due to various dynamical phenomena such as (a) arrivals/departures of users, (b) user mobility, (c) changes in the channel conditions.

Our price adaptation algorithm approximates the function F_p with a concave polynomial of second degree $g_p(\mathbf{x}) = \mathbf{x}^T\mathbf{A_p}\mathbf{x} + \mathbf{k_p}^T\mathbf{x} + v$ and estimates its parameters based on the history of the game evolution. Specifically, each provider maintains a dataset

$$D_p = \{\mathbf{x}(i), F_p(\mathbf{x}(i))\}_{i=n-M_p,\ldots,n-1,n} \quad (4)$$

where $\mathbf{x}(i)$ represents the ith combination of prices that has been offered in the market and M_p corresponds to the number of previous price combinations that are stored in the dataset D_p. To compute the parameters of the polynomial $g_p(\mathbf{x})$ each provider solves the following optimization problem.

$$\begin{aligned}\underset{\mathbf{A}_p,\mathbf{k}_p,v}{\text{minimize}} \quad & \sum_{i=n-M_p}^{n} w^{n-i}(g_p(\mathbf{x}(i)) - F_p(\mathbf{x}(i)))^2 \\ \text{subject to} \quad & g_p(\mathbf{x}) = \mathbf{x}^T\mathbf{A}_p\mathbf{x} + \mathbf{k}_p^T\mathbf{x} + v \\ & \mathbf{A}_p \preceq 0\end{aligned} \quad (5)$$

Where w takes a value between 0 and 1 and defines the weight with which previous price combinations are taken into consideration.

The above optimization problem is a semi-definite program and can be solved efficiently [16] . We constrain our polynomial to be concave for two reasons (a) to better capture the characteristics of concave payoff functions, and (b) to ensure the stability of the price adaptation process that is performed according to the following derivative rule.

$$x_p(n+1) = x_p(n) + \mu\left.\frac{\partial g_p(\mathbf{x})}{\partial x_p}\right|_{\mathbf{x}=\mathbf{x}(n)} \quad (6)$$

where μ is the step size.

To initialize our algorithm, we take into consideration that the price 0 corresponds to revenue 0 for all providers. Moreover, each provider starts by offering a very small price (0.01 in our simulations). The initial estimation of the polynomial parameters is based on these first observations. Due to the limited number of available points in the dataset D_p, at the beginning of the experiment, the solution of the problem (5) may require a large number of Newton steps. In this case, we restrict the number of steps to be lower than a threshold. This leads a crude initial estimation of the polynomial that is improved as the size of the dataset increases.

Alternatively, we could initialize our algorithm by solving a least-norm problem (minimize the Euclidean norm of the vector that contains the polynomial parameters) instead of a least-squares problem until the size of the dataset D_p becomes larger than the number of the polynomial parameters.

Finally, at the beginning of the experiment, the polynomial parameters are re-estimated every time a provider $p \in P$ adds a new point to the dataset D_p. When the size of the dataset becomes larger than a threshold, the parameters of the polynomial are renewed once for every L (in our simulations 10) new points that are added to the dataset D_p. This decreases the computational complexity of the algorithm. The price adaptation is still based on the rule (6) using the most recent estimation of the polynomial.

III. Performance Evaluation

A. Scenario description

Two cellular networks, deployed by different providers, offer services to users in a small city, represented as a rectangle of 11 Km x 9 Km. Each network consists of 49 BSs placed on the sites of a triangular grid, with a distance between two neighboring sites of 1.6 Km. Moreover, each provider owns bandwidth of 5.6 MHz, that is divided into 28 channels of 0.2 MHz width. These channels are allocated to BSs according to a frequency reuse scheme with spatial reuse factors 4 and 7, for Provider 1 and Provider 2, respectively. To find the closest interferers of a particular BS when the spatial reuse factor is 4, we move two steps towards any direction on the grid. On the other hand, when the spatial reuse factor is 7, we move two steps towards any direction and then we turn 60 degrees and move one more step. This is illustrated in Fig. 1. Each channel is further divided into three time-frequency slots in a TDMA scheme, resulting in 21 time-frequency slots per BS of Provider 1 and 12 slots per BS of Provider 2. Note that a single time-frequency slot can be offered to only one user. Also the user demand is exactly one slot.

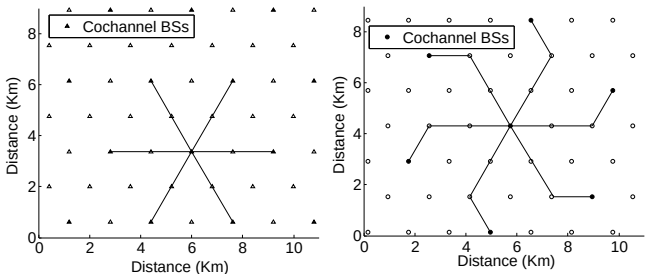

(a) (b)

Fig. 1: Closest interfering BSs when the reuse factor is 4 (left) and 7 (right).

There is a distribution of 600 users in this region interested in buying Internet access from these two providers. Each user can "tolerate" a maximum cost for the Internet access (i.e., *price-tolerance* threshold), given by a Gaussian distribution (0.15, 0.014) and has a *target transmission rate* (expressed in Mbps) that follows a Gaussian distribution (0.1, 0.0001).

A Uniform and a Zipf topology are simulated. In the Uniform topology, the users are distributed in the entire region according to a Uniform distribution. On the other hand, in the Zipf topology, 250 users are distributed uniformly in the entire region and the population of the remaining 350 users is split into five circular regions around the center of the city with radius of 2 Km each. The number of users that are placed in each circular region is determined by the Zipf's law with parameter s = 1 and the specific locations of users are determined according to a uniform distribution at each region. In both cases, users are stationary. Fig. 2 shows the Zipf topology.

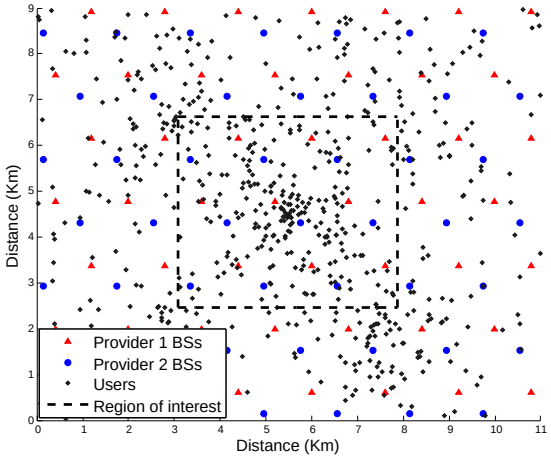

Fig. 2: Zipf-like distribution of users in a small city

To avoid the effect of various boundary conditions, we analyzed only the measurements collected in a small rectangular region at the center of the city (shown as the inner rectangle in Fig. 2, marked as "region of interest"). Specifically, *only* the BSs located in that region and users of that region that also access the Internet via those BSs are considered in the price adaptation algorithm and in the reported evaluation results. The region of interest includes 9 BSs of each provider. 150 users are present in the Uniform topology and 242 users in the Zipf topology, respectively.

Two user-preference metrics were simulated, namely the *transmission-rate* and *price-preference* ones. In rate preference, users take into consideration *only* the achievable transmission rate, given that the offered price from the specific BS does not exceed their price-tolerance threshold. Users with price preference aim to minimize the cost of acquiring a time-frequency slot, given that their target transmission rate requirement is satisfied. Each user reconsiders its choice periodically (here, every 2 sec), while each provider adapts its price at time instances produced by a Poisson process with a mean of 0.03 renewals/sec. Providers run the price adaptation algorithm described in Section II. An experiment corresponds to a specific topology (Uniform "U" or Zipf "Z") and all its users employ the same user preference metric (Price "P" or Rate "R" preference). It lasts for 2000 sec. The results reported for each scenario (e.g., "U-R"in Fig.4, for a Uniform topology with rate preference) are average statistics over 30 Monte Carlo runs. This simulation testbed was implemented in Matlab.

B. Simulation results and discussion

In rate-preference, a user connects to the BS that offers the best channel in terms of received SINR. Due to the spatial reuse scheme, the impact on SINR of the interference of other users at co-channel cells is relatively small compared to the channel gain, which is determined mostly by the distance between transmitter (a given user) and receiver (its BS). Therefore, users tend to select the geographically nearest BS. This has as a result providers to increase their prices, without *significantly* influencing the BS selection process of users. Consequently, the prices of the two providers converge to a relatively high value compared to the average price tolerance threshold of users.

On the contrary, in price preference, users connect to a BS of the least expensive provider, given that they can still achieve their target transmission rate. In these scenarios, even small changes in the price could cause some users to change provider. This has two important implications; First, compared to the rate-preference scenario, a larger number of handoffs are performed between BSs of the two providers. Second, the intensity of competition keeps the prices of the two providers at relatively low levels.

Fig. 3 presents the evolution of prices under the two topologies and user preference metrics, while Fig. 4 summarizes the revenue and spectrum utilization *per BS* for each provider and the number of handoffs and percentage of disconnection of users. Specifically, the revenue corresponds to the average of the total revenue of all BS at the region of interest throughout an experiment, averaged over all Monte-Carlo runs. The spectrum utilization for a BS is the integral of the percentage of time slots assigned to users during the experiment, normalized by the duration of the experiment. The reported value is computed in the same manner as the revenue. The number of handoffs corresponds to the number of transitions between BSs of a user during an experiment, averaged over all users and all Monte-Carlo runs. The disconnection period of a user corresponds to the total percentage of time that this user is disconnected during an experiment. We compute the average over all users in an experiment, and report the average over all Monte-Carlo runs.

The spatial user distribution affects the system dynamics: In the uniform topology, the total number of users located in the region of interest is 150. Furthermore, the availability of time-frequency slots of the two providers is 189 and 108, respectively. Therefore, the provider 2 is not able to satisfy the user demand, resulting to a small advantage for the provider 1 in terms of number of clients and revenue. On the contrary, in the Zipf topology, the user population in the region of interest is 242 and their demand exceeds the availability of time-frequency slots of each provider. Thus, the providers in Zipf have the opportunity to increase their prices even further, resulting in higher revenues for both providers (compared to the Uniform topology). Finally, due to the high user density, the difference in the revenue of the two providers increases (compared to what was observed in the Uniform topology). The above results are shown in Fig.4 (a).

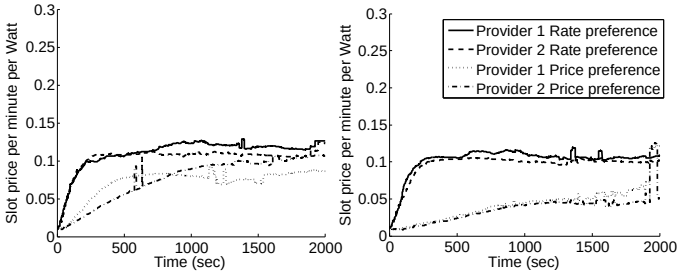

Fig. 3: The price evolution in Zipf (left) and Uniform (right) topologies.

In price-preference, the prices are higher in the Zipf topology. This is because the user demand is larger than the availability of time frequency slots of each provider. This offers more opportunities for price increase than in the uniform topology. In rate-preference, the prices in the two topologies are similar (U-R vs. Z-R), since users decide based on topological criteria. The price evolution is mostly affected by the user price tolerance threshold which follows the same distribution in both topologies.

The revenue is higher in rate-preference than in price-preference scenarios, not only due to the higher prices but also, since users tend to invest more transmission power to achieve higher rate. Finally, the spectrum utilization is higher for the Provider 2, due to its lower availability of time-frequency slots.

As observed earlier, compared to rate-preference, the price-preference corresponds to a larger number of handoffs (e.g., U-R vs. U-P, and Z-R vs. Z-P). However, exactly the opposite occurs for the disconnection intervals. In rate preference, the prices are higher than in price preference, exceeding the price tolerance thresholds of a larger number of users.

Interestingly, in the Uniform topology, a larger number of handoffs and lower disconnection periods occur. This is due to the lower user demand in the Uniform topology than in the Zipf topology (150 vs. 242 users), resulting to a larger availability of time-frequency slots. Thus, the likelihood that a user will be able to connect to a BS is higher in the Uniform topology than in the Zipf one. This means that a user has on average more opportunities to roam to a different network. On the contrary, in Zipf, the likelihood of fully-utilized time-frequency slots of BSs is higher, resulting to fewer choices for users, and thus, longer disconnection periods.

Finally, the median value of handoffs and disconnection periods is much lower that the corresponding mean values, indicating that most users are connected to a single BS for the entire experiment. A small number of users switch back and forth between BSs or remain disconnected for almost the entire duration of the experiment.

IV. Conclusions and future work

This report presents a microscopic spatial and temporal scale of the interactions between cellular network providers and users. It analyzes the impact of topology and price and rate

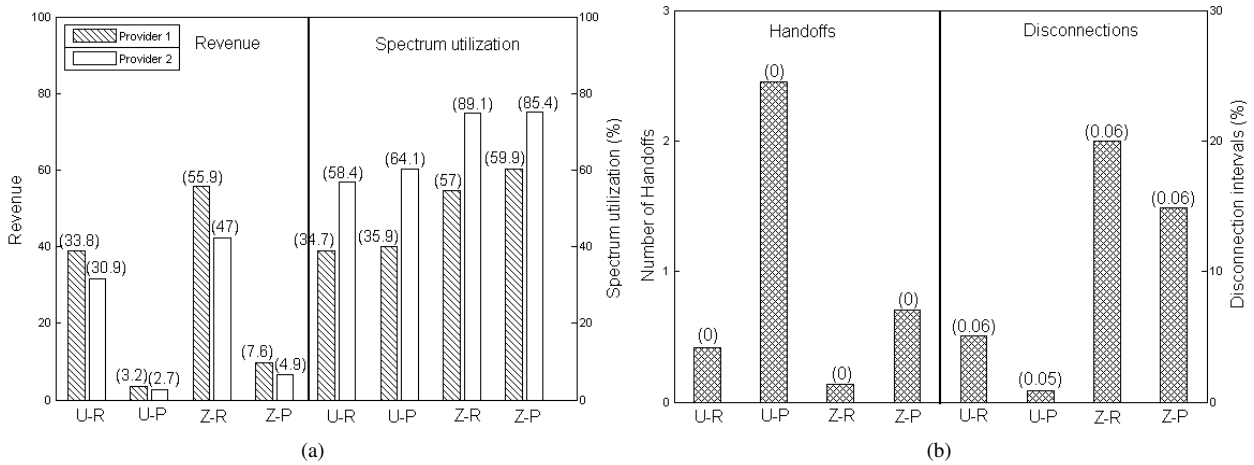

Fig. 4: (a) Provider revenue (left) and spectrum utilization (right), (b) User handoffs (left) and disconnection intervals (right).

preference on the price evolution, provider revenue, spectrum utilization, number of handoffs and disconnection periods. It also highlights the effect of price tolerance and preference on the degree of competition between providers. It is possible under different BS deployments, user distributions, population sizes, and preferences to observe phenomena like price wars and monopolies. Furthermore, it is part of future work to explore how these interactions evolve in larger spatio-temporal scales.

In this work, users select the appropriate BS (and provider) based on their current observations/measurements of the channel quality and price. A part of our on-going effort focuses on modeling other novel schemes, such as the integration of their previous measurements ("history") or available community-based measurements (collected from various devices) to enhance the network/provider selection process. Moreover, this work considers user utility functions based on the channel capacity (a measure of the maximum achievable transmission rate). However, we plan to incorporate user-centric functions that take into consideration finer-level statistics on network conditions and reflect the user satisfaction.

Another prominent feature of our research is the design and integration of spectrum-sharing mechanisms that will realize various competitive, cooperative, and hybrid business models. Such models will be instantiated using specific parameters of the proposed framework (e.g. the amount of information shared among various entities and type of interaction) and access paradigms that depict realistic business cases. For example, in a cooperative business model, cellular networks may establish long-term agreements with TV networks or network providers of IEEE802.11 infrastructures form coalitions. We believe that this work sets the directions for developing a general framework that allows researchers to instantiate, implement, and assess interesting and realistic spectrum-based market approaches.

REFERENCES

[1] S. Hwang, M. Katsoulakis, and L. Rey-Bellet, "Deterministic Equations for Stochastic Spatial Evolutionary Games," *ArXiv e-prints*, Jul. 2010.

[2] A. Al Daoud, T. Alpcan, S. Agarwal, and M. Alanyali, "A stackelberg game for pricing uplink power in wide-band cognitive radio networks," in *47th IEEE Conference on Decision and Control*, 2008.

[3] F. Fu and M. van der Schaar, "Learning to compete for resources in wireless stochastic games," *IEEE Transactions on Vehicular Technology*, vol. 58, no. 4, pp. 1904 –1919, may. 2009.

[4] D. Niyato and E. Hossain, "Competitive spectrum sharing in cognitive radio networks: a dynamic game approach," *Wireless Communications, IEEE Transactions on*, vol. 7, no. 7, pp. 2651 –2660, 2008.

[5] F. Wang, M. Krunz, and S. Cui, "Price-based spectrum management in cognitive radio networks," *Selected Topics in Signal Processing, IEEE Journal of*, vol. 2, no. 1, pp. 74 –87, 2008.

[6] L. Gao, X. Wang, Y. Xu, and Q. Zhang, "Spectrum trading in cognitive radio networks: A contract-theoretic modeling approach," *IEEE Journal on Selected Areas in Communications*, vol. 29, no. 4, 2011.

[7] H. Yu, L. Gao, Z. Li, X. Wang, and E. Hossain, "Pricing for uplink power control in cognitive radio networks," *Vehicular Technology, IEEE Transactions on*, vol. 59, no. 4, pp. 1769 –1778, May 2010.

[8] T. Wysocki and A. Jamalipour, "Pricing of cognitive radio rights to maintain the risk-reward of primary user spectrum investment," in *IEEE Dyspan*, 2010.

[9] J. Jia, Q. Zhang, Q. Zhang, and M. Liu, "Revenue generation for truthful spectrum auction in dynamic spectrum access," in *MobiHoc*, New York, NY, USA, 2009.

[10] J. Jia and Q. Zhang, "Competitions and dynamics of duopoly wireless service providers in dynamic spectrum market," in *MobiHoc*, 2008, pp. 313–322.

[11] J. W. Mwangoka, K. B. Letaief, and Z. Cao, "Joint power control and spectrum allocation for cognitive radio networks via pricing," *Physical Communication*, vol. 2, no. 1-2, pp. 103 – 115, 2009.

[12] D. Niyato and E. Hossain, "Competitive pricing for spectrum sharing in cognitive radio networks: Dynamic game, inefficiency of nash equilibrium, and collusion," *Selected Areas in Communications, IEEE Journal on*, vol. 26, no. 1, pp. 192 –202, jan. 2008.

[13] K. Pahlavan and A. H. Levesque, *Wireless information networks*. New York, NY, USA: Wiley-Interscience, 1995.

[14] M. Gudmundson, "Correlation model for shadow fading in mobile radio systems," *Electronics Letters*, vol. 27, no. 23, pp. 2145 –2146, 1991.

[15] I. Forkel, M. Schinnenburg, and M. Ang, "Generation of two-dimensional correlated shadowing for mobile radio network simulation," in *WPMC*, Sep 2004.

[16] S. Boyd and L. Vandenberghe, *Convex Optimization*. New York, NY, USA: Cambridge University Press, 2004.